A Spectral Method for 3D Shape Reconstruction and Denoising

Alfred Hero and Jia Li

University of Michigan
Ann Arbor, MI 48109
http://www.eecs.umich.edu/~hero/

Outline

- Polar shape modeling
- KLE representations for polar shape
- Spectral methods for registration/reconstruction
- Spectral methods for active contours

Motivation

- Why shape modeling?
  - Object recognition
  - Shape recovery
  - Medical image analysis
    - Medical training
    - Clinical application

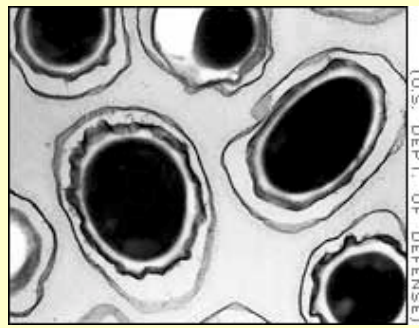

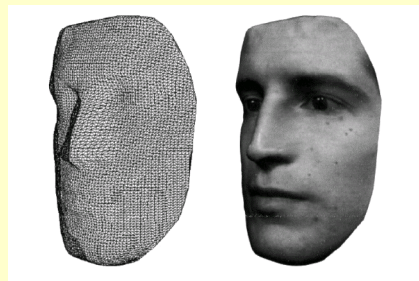

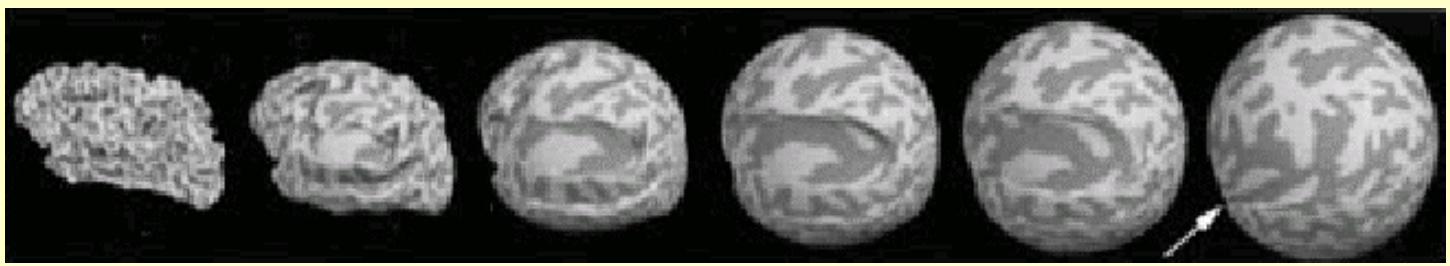

3D Polar Surfaces

- 3D surface $\mathbf{X}$

$$\mathbf{X}(u,v) = [x_1(u,v), x_2(u,v), x_3(u,v)];$$

$$(u,v) \in \Omega, \qquad \Omega \subset R^2$$

- Star-shaped (polar) surface $r(\theta,\phi)$

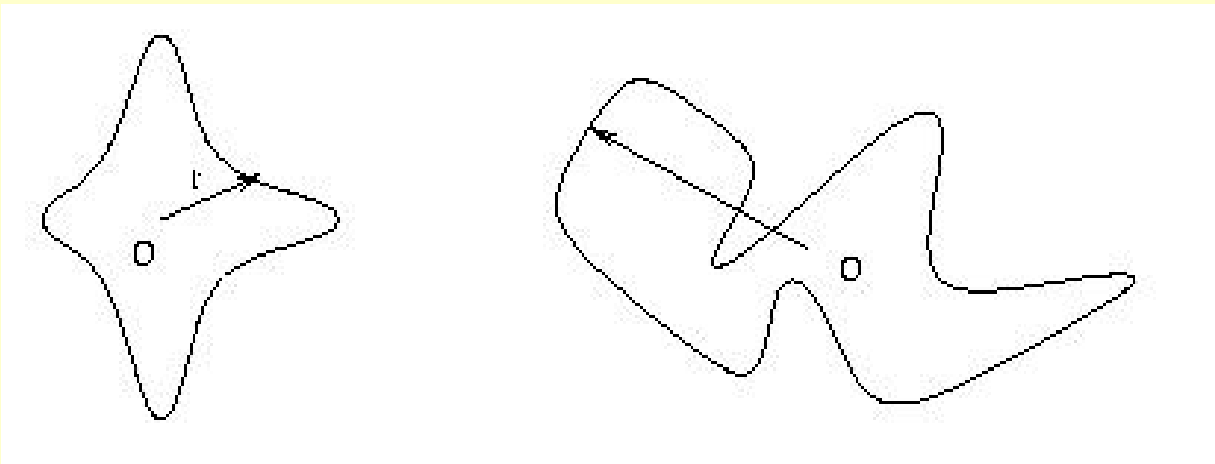

Spherical Coordinate System

ϕ azimuth

θ elevation

$r(\theta, \phi)$

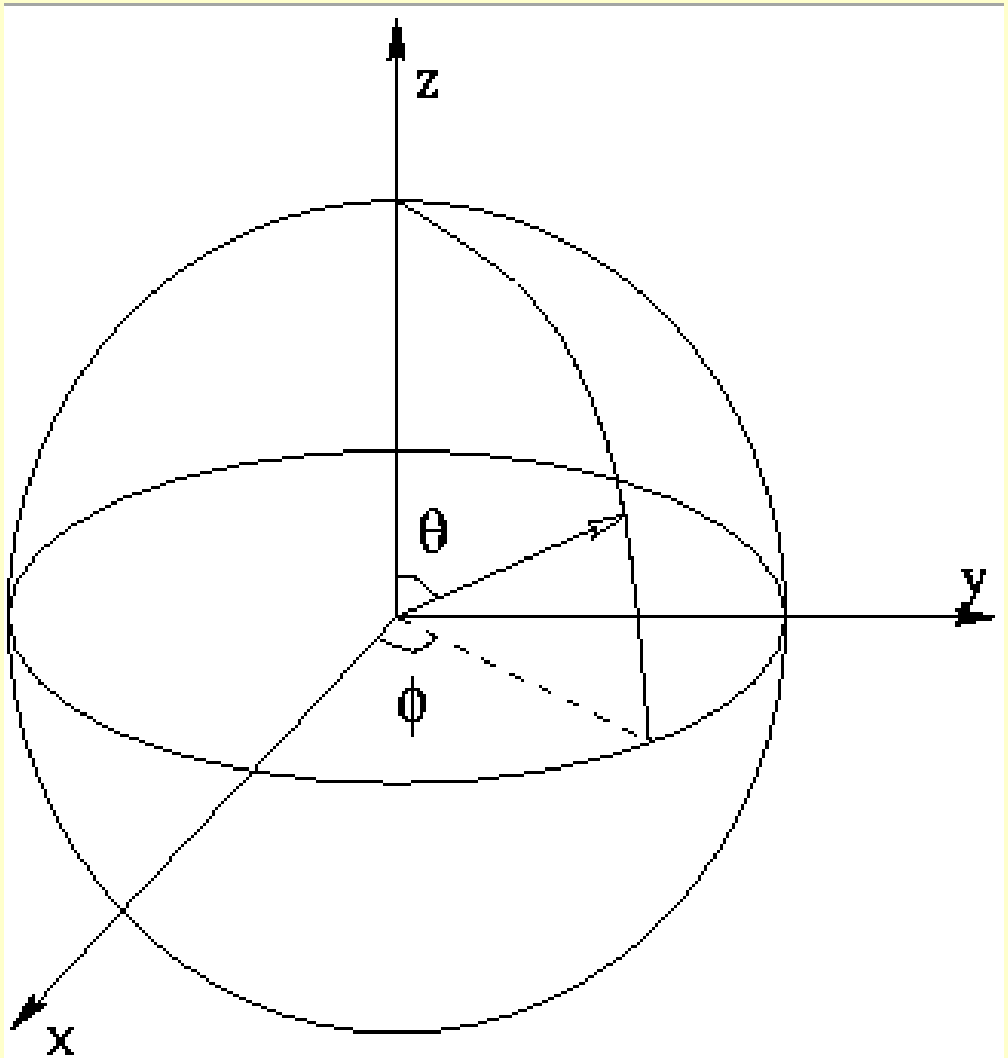

3D Fourier Descriptors

$$f(\theta,\phi) = \sum_{m=-\infty}^{\infty} f_m(\theta) e^{im\phi}$$

- Orthonormal basis
- Complete basis
- Ordered in increasing spatial frequency
- Common expansion in azimuth (longitude)

Spherical Harmonics

$$Y_l^m(\theta,\phi) = \underbrace{(-1)^m \sqrt{\frac{2l+1}{4\pi}\frac{(l-m)!}{(l+m)!}} P_l^m(\cos\theta)}_{f_{m,l}(\theta)} e^{im\phi}$$

- Angular solutions of Laplace equation on sphere
- Karhunen-Loeve basis for isotropic random field
- Requires computation of Legendre polynomials
- Applied to shape approximation (Haigron&etal:98, Danielsson&etal:ICPR98, Matheny&etal:PAMI95)
- Implementation: SVD or FFT algorithm

First 10 Spherical Harmonics

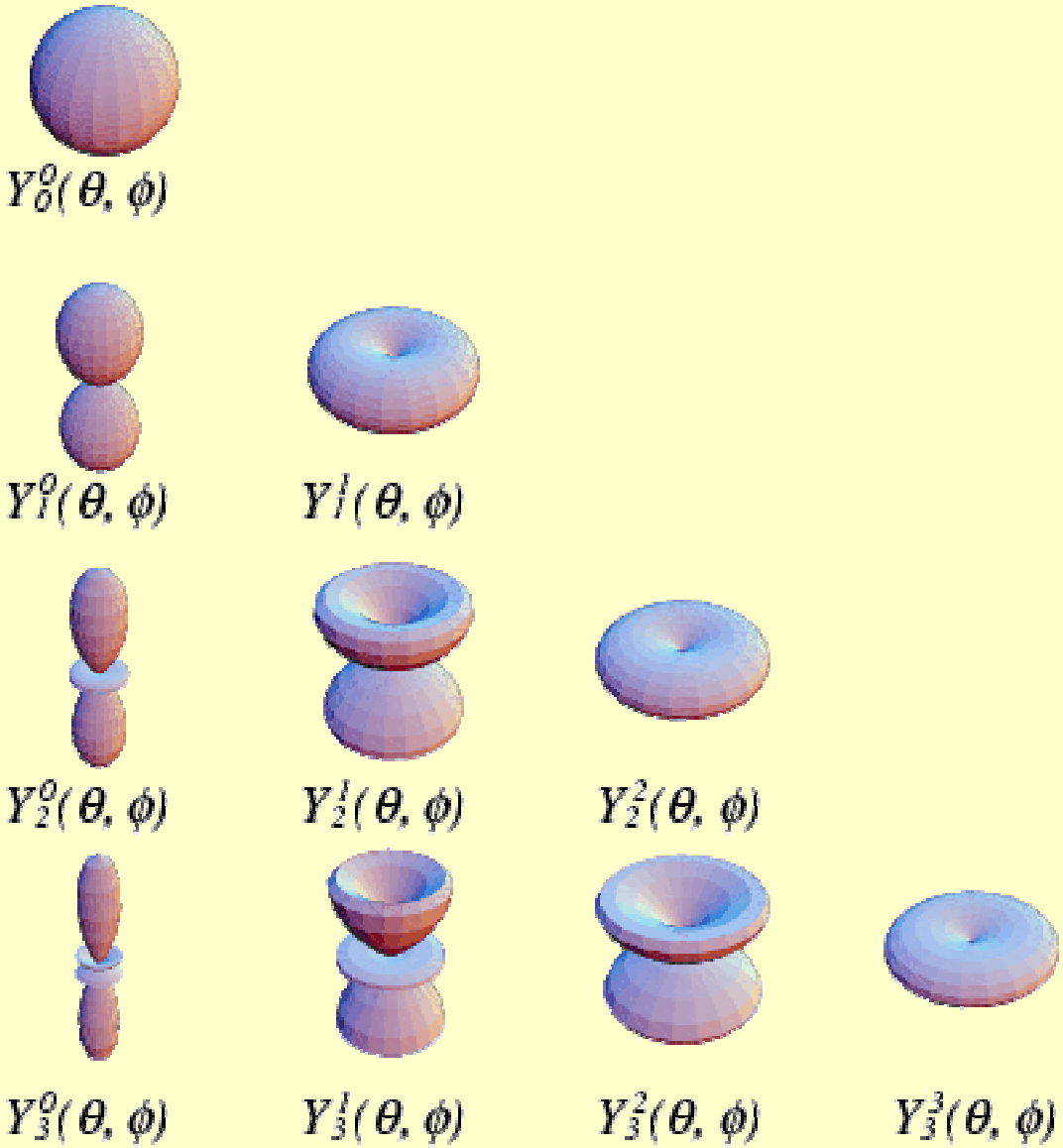

Computing Spherical Harmonic Coefficients

- GaussElim/SVD method via optimized sampling (Erturk&Dennis:ElectLett97, Matheny:PAMI95)

  $(K+1)^2$ unknown coefficients C

$$R(\theta,\phi)=\sum_{l=0}^{K}\sum_{m=-l}^{l}A_l^m U_l^m(\theta,\phi)+B_l^m V_l^m(\theta,\phi)$$

$$\mathbf{R}=\mathbf{UA}+\mathbf{VB}\Rightarrow\mathbf{R}=\mathbf{XC}$$

- Spherical FFT (Driscoll&etal:AdvAppMath94,Healy&etal:ICASSP96)
  - orthogonal discrete approximation to SH
  - lower complexity than SVD method
  - requires equi-spaced samples in azimuth/elevation

SH Numerical Comparisons

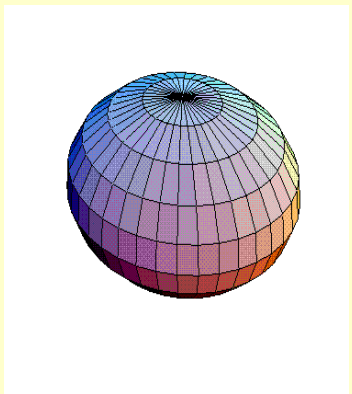

$$\left(\frac{x}{10}\right)^2+\left(\frac{y}{9}\right)^2+\left(\frac{z}{7}\right)^2=1$$

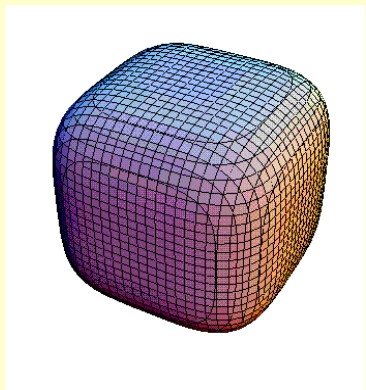

$$x^4+y^4+z^4=1$$

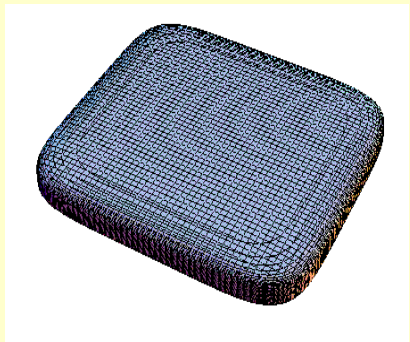

$$\left(\frac{x}{10}\right)^6+\left(\frac{y}{9}\right)^6+z^6=1$$

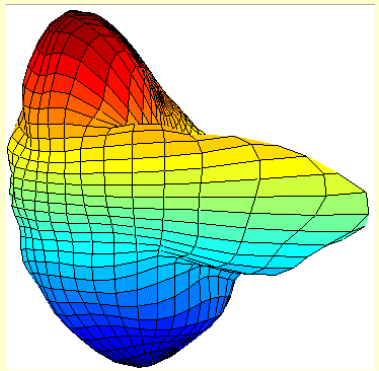

Liver Surface

3D Shapes used in the simulation

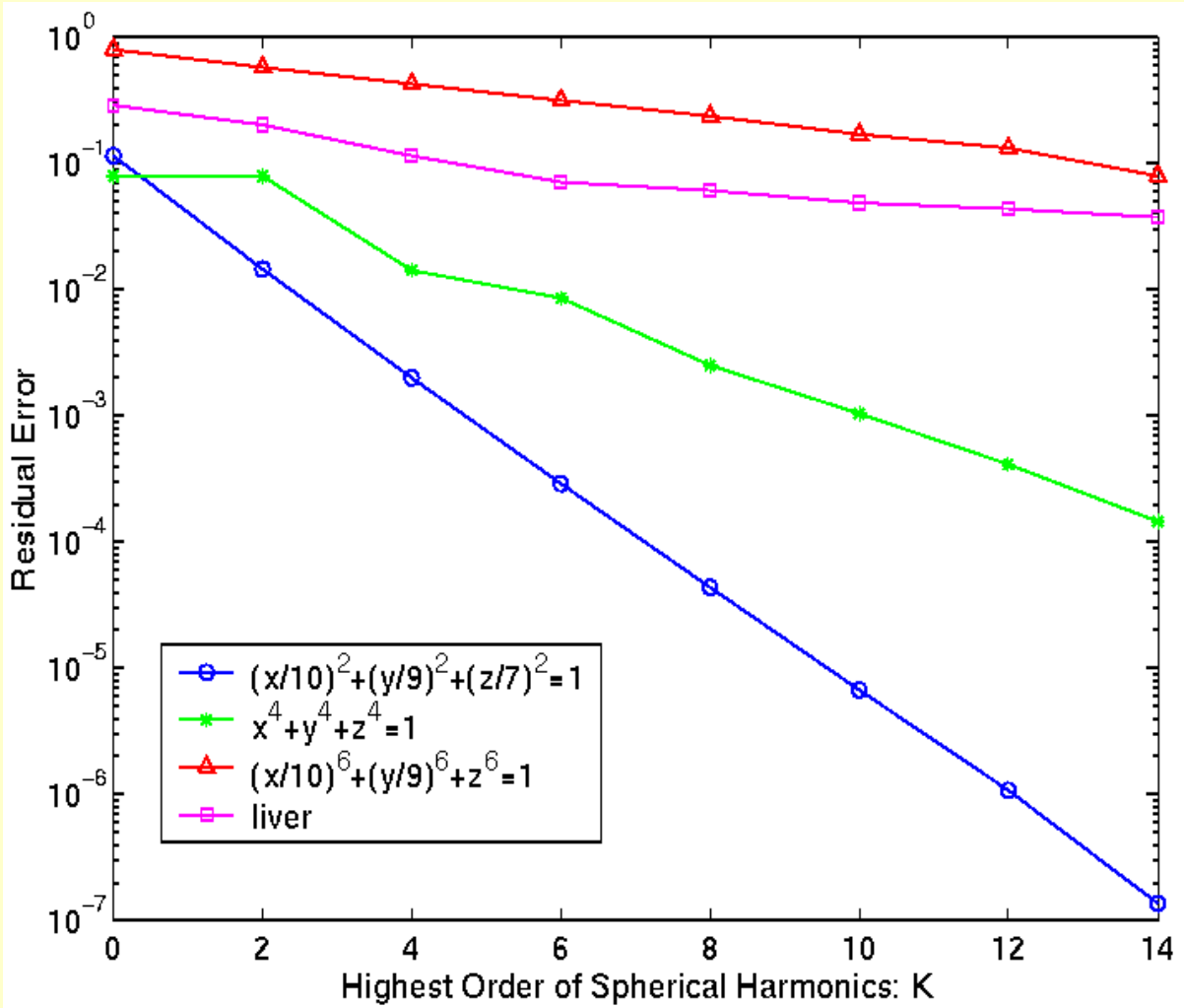

Shape modeling error vs. the highest order of spherical Harmonics for the four different shapes.

Double Fourier Series

- DFS are easier to manipulate than SH
- DFS over the sphere is more difficult than over R^2
- Boundary conditions for $f_m(\theta)$ at spherical poles

$$f_m(\theta) = \begin{cases} finite, & m = 0 \\ 0, & m \neq 0 \end{cases}$$

$$\frac{d}{d\theta} f_m(\theta) = \begin{cases} finite, & \text{odd } m \\ 0, & \text{even } m \end{cases}$$

- Standard 2D trigonometric series not admissible!
- Are there interesting admissible bases besides SH?

Admissible DFS Expansion

$$f_m(\theta) = \sum_{n=0}^{J-1} f_{n,0} \cos n\theta, \quad m = 0$$

$$f_m(\theta) = \sum_{n=1}^{J} f_{n,m} \sin n\theta, \quad \text{odd } m,$$

$$f_m(\theta) = \sum_{n=1}^{J} f_{n,m} \sin\theta \sin n\theta, \quad \text{even } m \neq 0.$$

Fourier coefficients can be computed using fast sin and cos transform

(Ref: Cheong:JournCompPhysics00)

SH vs DFS: Comparison

Metasphere surface

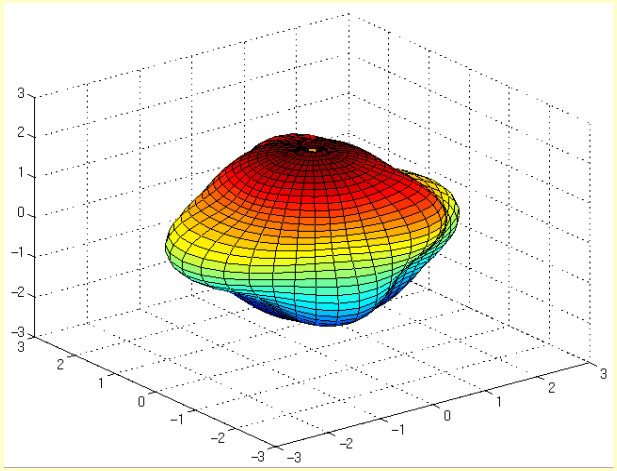

SH

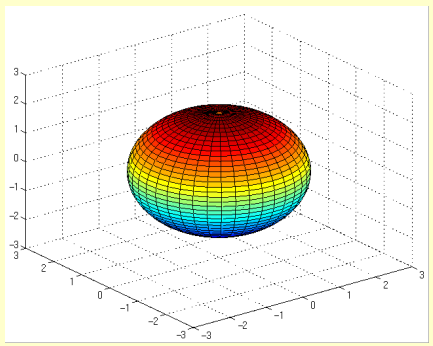

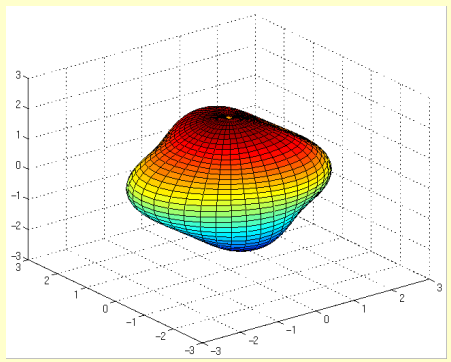

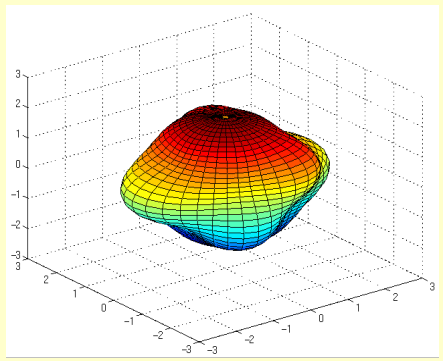

DFS

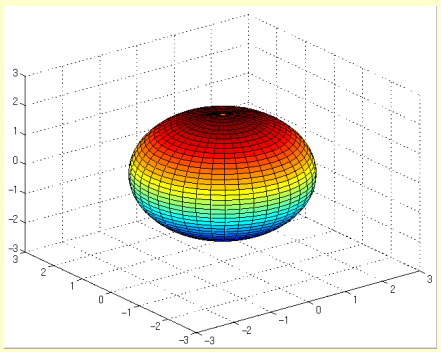

1 coeff

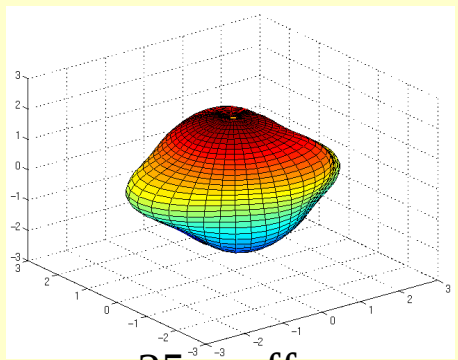

25 coeff

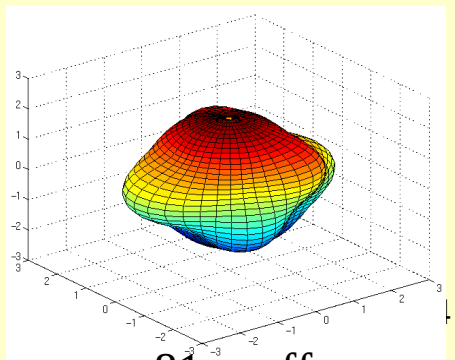

81 coeff

Statistical Polar Shape Modeling

- Common procedure
  - Extract shape features or parameters
    - Landmarks (Cootes CVIU95 &Frangi proc.Ipmi01)
    - SH coefficients (Staib PAMI96)
    - Distance map (Leventon proc. CVPR 00)
  - Compute mean and covariance of shape parameters.
  - Principle component analysis
  - Incorporate into other image processing algorithms
- Random field model

Decomposition of Isotropic Random Fields Over Unit Sphere Using SH

- Isotropic polar field satisfies

$$E\left\{X(\theta_1,\phi_1)X^*(\theta_2,\phi_2)\right\}=R(\gamma)=\psi(\cos\gamma)$$

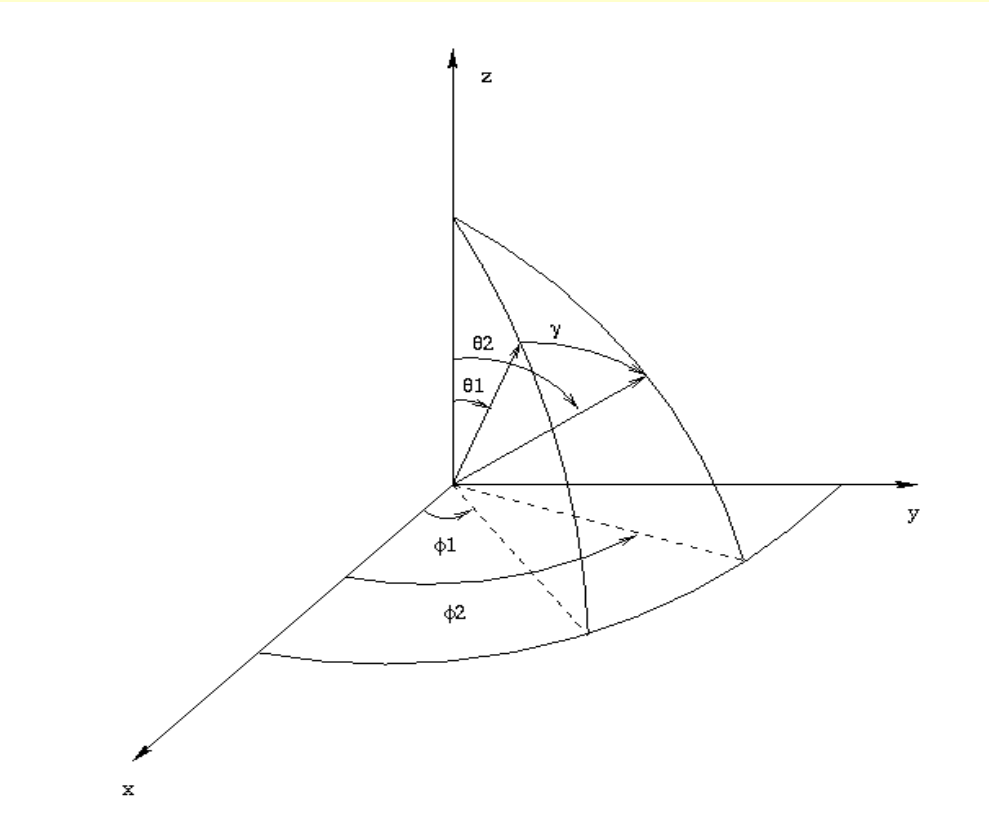

Karhunen-Loeve Expansion

SH are eigenfunctions of isotropic r.f. on sphere (Yadrenko:76)

$$X(\theta,\phi) = \sum_{l=0}^{\infty} \sum_{m=-l}^{l} A(l,m) Y_l^m(\theta,\phi)$$

$$A(l,m) = \int_{S^2} X(\theta,\phi) Y_l^{m*}(\theta,\phi) d\Omega$$

$$E\{A(l,m)\} = 0$$

$$E\{A(l,m) A^*(l',m')\} = \lambda_l \delta_{l,l'} \delta_{m,m'}$$

$$\lambda_l = 2\pi \int_{-1}^{1} \psi(t) P_l(t) \mathrm{d}t$$

Advantages of SH/DFS for Polar Shape Modeling

- A true frequency domain method over the unit sphere
- Low order basis smooth-fit segmented boundary
- Multiresolution structure can be used to iteratively recover higher frequencies
- Fast FFT methods can be implemented at each resolution via Driscoll&Healy or Cheong algorithm
- Orthogonal representation of isotropic random field model

Registration/Reconstruction

- Rotation $g \in SO(3)$
- Euler angles (α, β, γ)
- SH representations:

$$R(\theta,\phi) = \sum_{l=0}^{K} \sum_{m=-l}^{l} c_l^m Y_l^m(\theta,\phi) \qquad \text{(reference)}$$

$$\tilde{R}(\theta,\phi) = \sum_{l=0}^{K} \sum_{m=-l}^{l} \tilde{c}_l^m Y_l^m(\theta,\phi) \qquad \text{(rotated reference)}$$

$$\tilde{c}_l^m = \sum_{m'=-l}^{l} D^l_{mm'}(\alpha,\beta,\gamma) c_l^{m'}$$

$$D^l_{mm'}(\alpha,\beta,\gamma) = \exp(-im\alpha) \cdot d^l_{mm'}(\beta) \cdot \exp(-im'\gamma)$$

Joint Registration of 3D Rotation and Spherical Harmonic Coefficients

- Gaussian model

$$c_l^m = a_l^m + \eta_l^m$$

$$\tilde{c}_l^m = \sum_{n=-l}^{l} D_{mn}^l(\alpha,\beta,\gamma) a_l^n + \tilde{\eta}_l^m$$

- Marginal coefficient likelihood functions

$$L_{c_l^m} = \exp\left(-(c_l^m - a_l^m)^2 / 2\sigma_l^2\right)$$

$$L_{\tilde{c}_l^m} = \exp\left(-(\tilde{c}_l^m - \sum_{n=-l}^{l} D_{mn}^l(\alpha,\beta,\gamma) a_l^n)^2 / 2\tilde{\sigma}_l^2\right)$$

- ML estimator:

$$\{\hat{\alpha},\hat{\beta},\hat{\gamma},\{\hat{a}_l^m\}\} = \underset{\alpha,\beta,\gamma,\{a_l^m\}}{\operatorname{argmin}} \sum_{l=1}^{K}\sum_{m=-l}^{l}\left(\frac{(c_l^m - a_l^m)^2}{\sigma_l^2} + \frac{(\tilde{c}_l^m - \sum_{n=-l}^{l} D_{mn}^l(\alpha,\beta,\gamma) a_l^n)^2}{\tilde{\sigma}_l^2}\right)$$

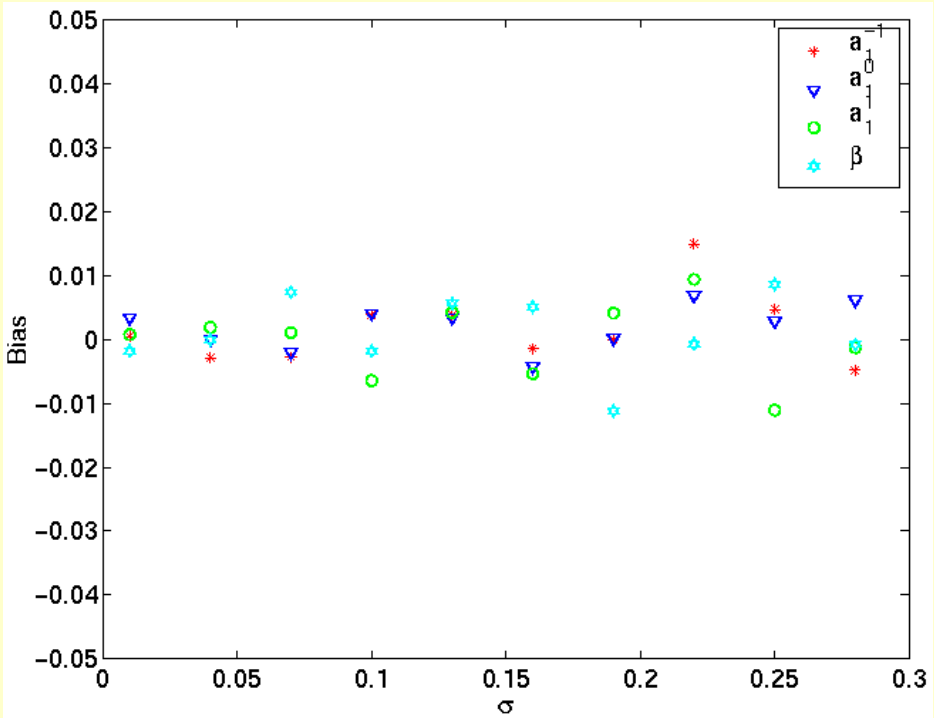

Bias

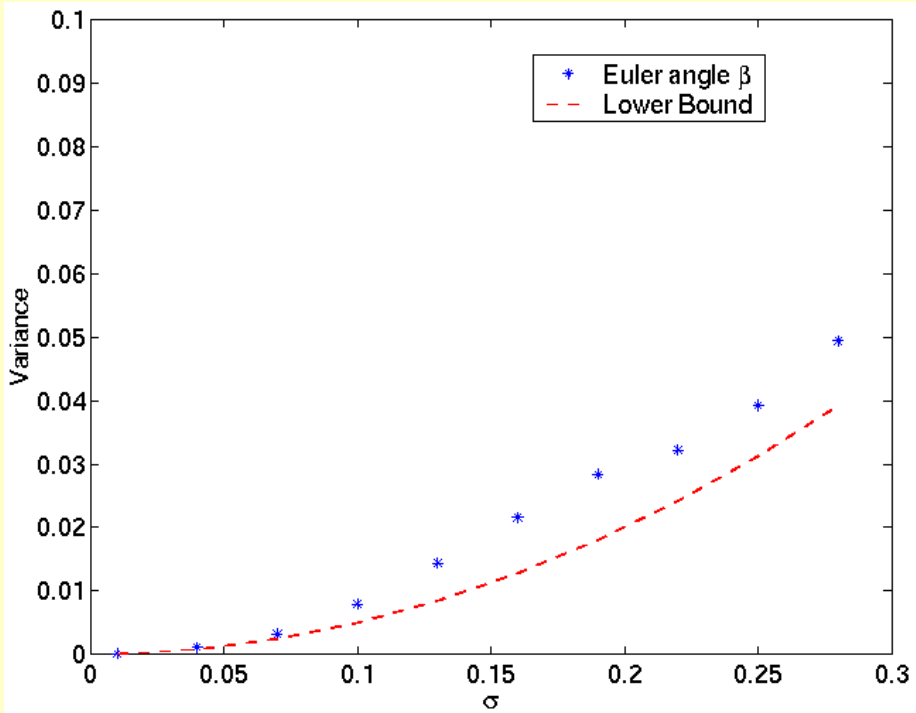

Variance and CR bound

The performance of the maximum likelihood estimator which jointly estimates the Euler angles and the shape parameters.

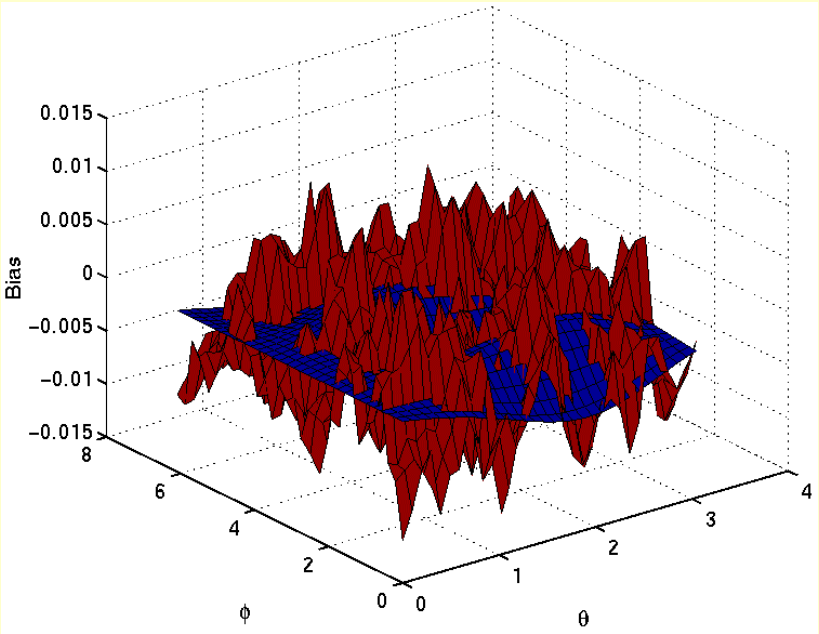

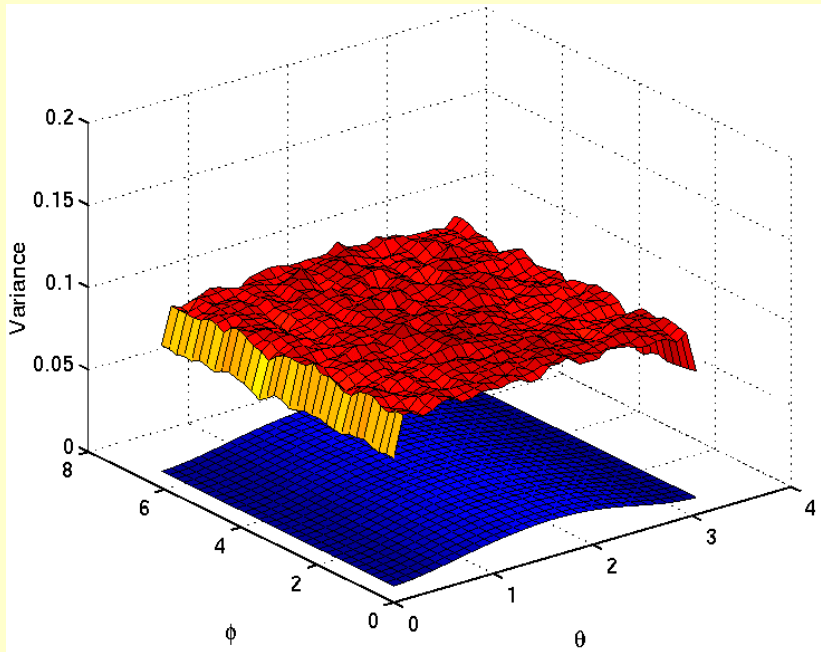

Bias and variance of radial reconstruction for
Lowpass(red) vs Weiner(blue) filtering

Application to Active Contour Surface Reconstruction

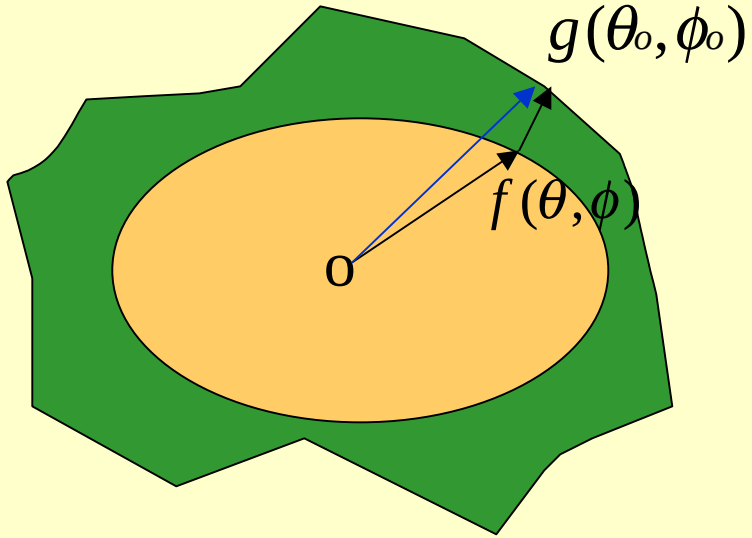

$$E(f) = \int_{S^2} ((f - g_f)^2 + \alpha \|\nabla f\|^2) d\Omega$$

α : non-negative roughness parameter

Polar Euler-Lagrange Equation

Minimizer f of E(f) must satisfy PDE over S^2

$$\alpha \nabla^2 f - (f - g_f)(1 - \frac{\partial g_f}{\partial f}) = 0$$

$$\nabla^2 = \frac{1}{\sin\theta}\frac{\partial}{\partial\theta}(\sin\theta\frac{\partial}{\partial\theta}) + \frac{1}{\sin^2\theta}\frac{\partial^2}{\partial\phi^2}$$

Front propagation consists of two steps:

At iteration n

1.Update f: $\alpha \nabla^2 f_{n+1} - f_{n+1} = -(f_n - g_{f_n})\frac{\partial g_{f_n}}{\partial f_n} - g_{f_n}$ (solve Helmholtz)

2.Update g: $g_{f_n} \rightarrow g_{f_{n+1}}$ (determine external force)

Methods of Solving Helmholtz

$$\nabla^2 f - \mu(f - g) = 0$$

- Iterative FEM and FDM
  - Advantage: non-uniform sampling can be accommodated
  - Disadvantage: very high computational complexity
- Non-iterative spectral methods
  - Spherical harmonic expansions
  - Double Fourier series

Comparison:

- Grid size $N \times N$
- Computational complexity
  - FEM/FDM Method $O(N^6) \sim O(N^3)$
  - New Spectral Method $O(N^2 \log N)$

Spectral Solution to Helmholtz

$$f(\theta,\phi) = \sum_{m=-\infty}^{\infty} f_m(\theta) e^{im\phi}$$

Fourier Descriptor

$$f_m(\theta) = \sum_{n=-\infty}^{\infty} f_{m,n} \cos(n\theta + n\pi/2)$$

Cheong's trig series

1. Substitute Fourier descriptor $f_m(\theta)$ into Helmholtz equation

$$\frac{1}{\sin\theta}\frac{d}{d\theta}(\sin\theta \frac{d}{d\theta} f_m(\theta)) - \frac{m^2}{\sin^2\theta} f_m(\theta) = \mu[f_m(\theta) - g_m(\theta)]$$

2. Substitute Cheong's expansion of $f_m(\theta)$

Helmholtz Recursions

$$\frac{(n-1)(n-2)+\mu}{4} f_{n-2,m} - \frac{n^2+2m^2+\mu}{2} f_{n,m} + \frac{(n+1)(n+2)+\mu}{4} f_{n+2,m}$$

$$= \mu\left(\frac{1}{4} g_{n-2,m} - \frac{1}{2} g_{n,m} + \frac{1}{4} g_{n+2,m}\right) \qquad m = 0, \text{ or odd}$$

$$\frac{n(n-1)+\mu}{4} f_{n-2,m} - \frac{n^2+2m^2+\mu}{2} f_{n,m} + \frac{n(n+1)+\mu}{4} f_{n+2,m}$$

$$= \mu\left(\frac{1}{4} g_{n-2,m} - \frac{1}{2} g_{n,m} + \frac{1}{4} g_{n+2,m}\right) \qquad m \text{ even and} \neq 0$$

After truncation obtain tridiagonal linear system

$$B\mathbf{f} = A\mathbf{g}$$

$$\begin{pmatrix} b_{1,m} & c_1 & & & & \\ a_3 & b_{3,m} & c_3 & & & \\ & \ddots & \ddots & \ddots & & \\ & & a_{J-3} & b_{J-3,m} & c_{J-3} & \\ & & & a_{J-1} & b_{J-1,m} & \end{pmatrix} \begin{pmatrix} f_{1,m} \\ f_{3,m} \\ \vdots \\ f_{J-3,m} \\ f_{J-1,m} \end{pmatrix} = \begin{pmatrix} 2 & -1 & & & & \\ -1 & 2 & -1 & & & \\ & \ddots & \ddots & \ddots & & \\ & & -1 & 2 & -1 & \\ & & & -1 & 2 & \end{pmatrix} \begin{pmatrix} g_{1,m} \\ g_{3,m} \\ \vdots \\ g_{J-3,m} \\ g_{J-1,m} \end{pmatrix}$$

1. $g(\theta,\phi) \rightarrow g_{n,m}$
2. Obtain $f_{n,m}$ by solving matrix equations
3. $f_{n,m} \rightarrow f(\theta,\phi)$

Experiment 1: Ellipsoidal Surface Reconstruction Different Regularization Parameter

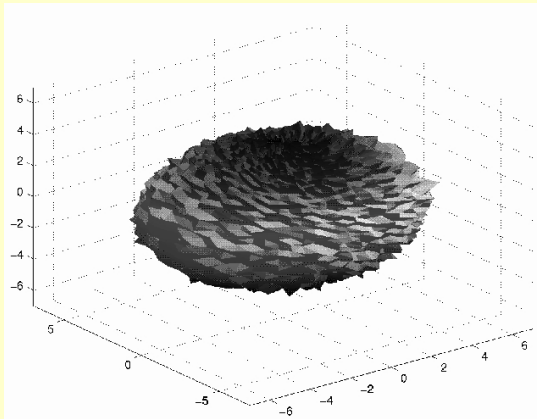

Original segmentation

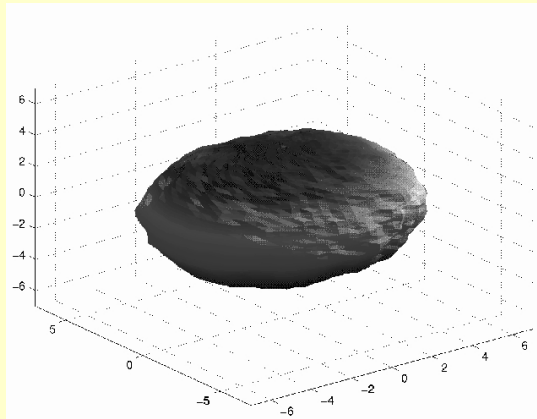

$\mu = 10^4$

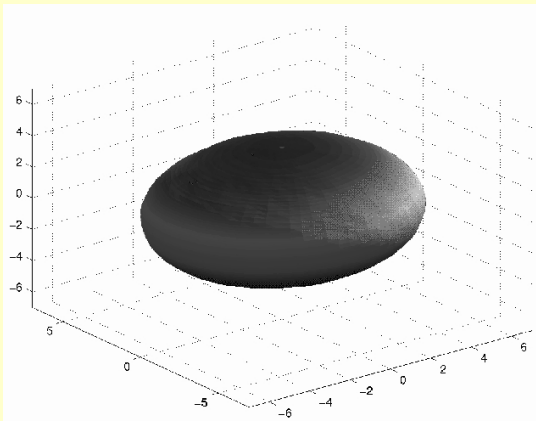

$\mu = 10^3$

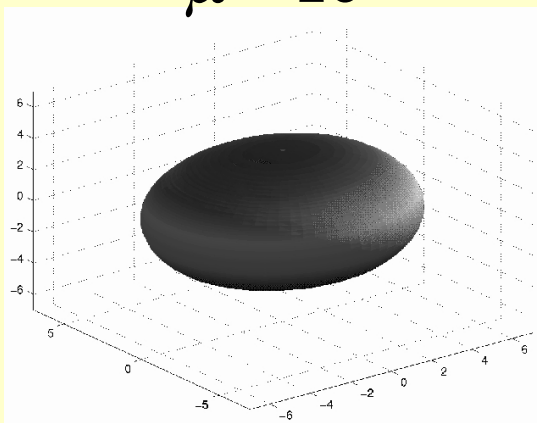

$\mu = 10^2$

Data Regularization Parameter

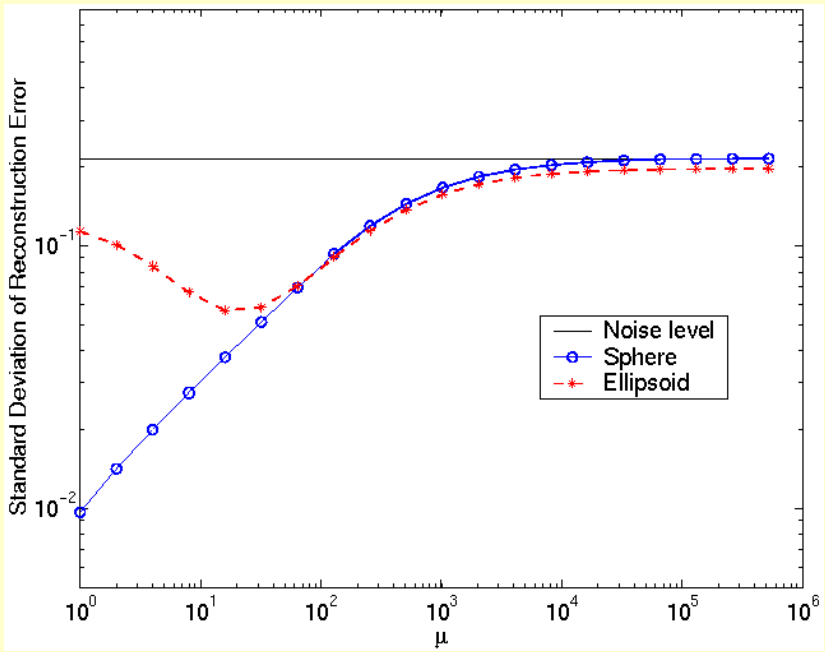

Different shapes

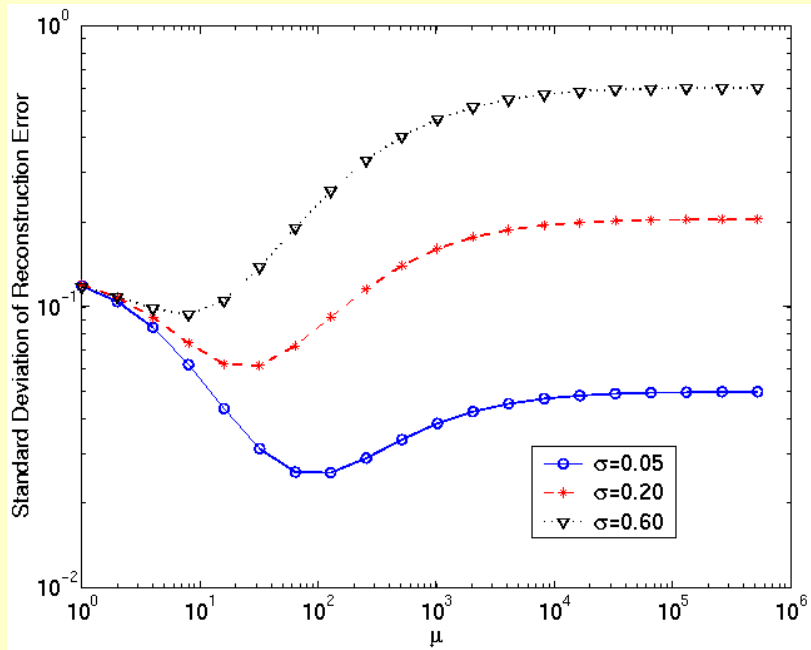

Different noise levels

Experiment 2: CT Thoracic Slices

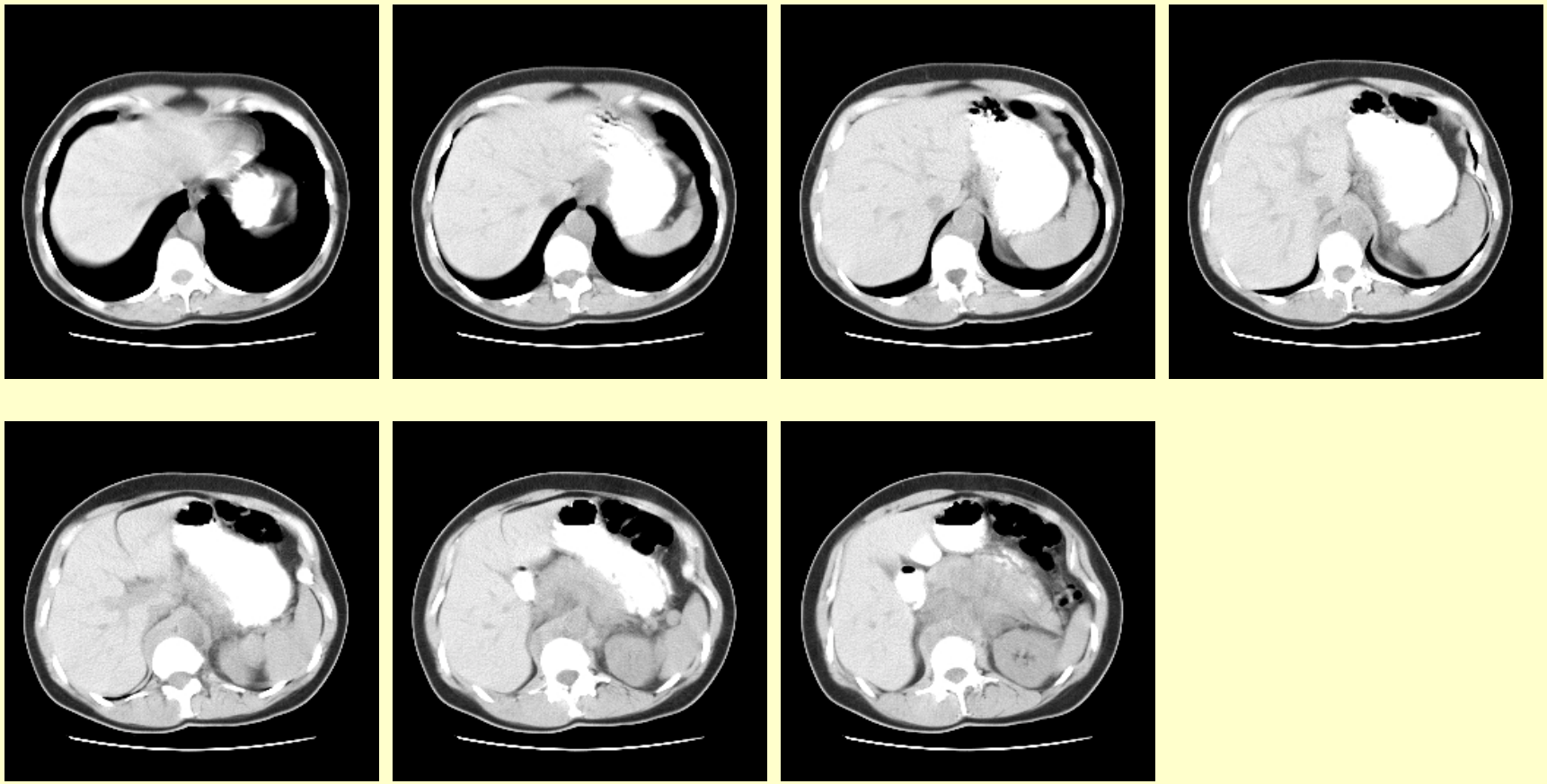

Edge-maps

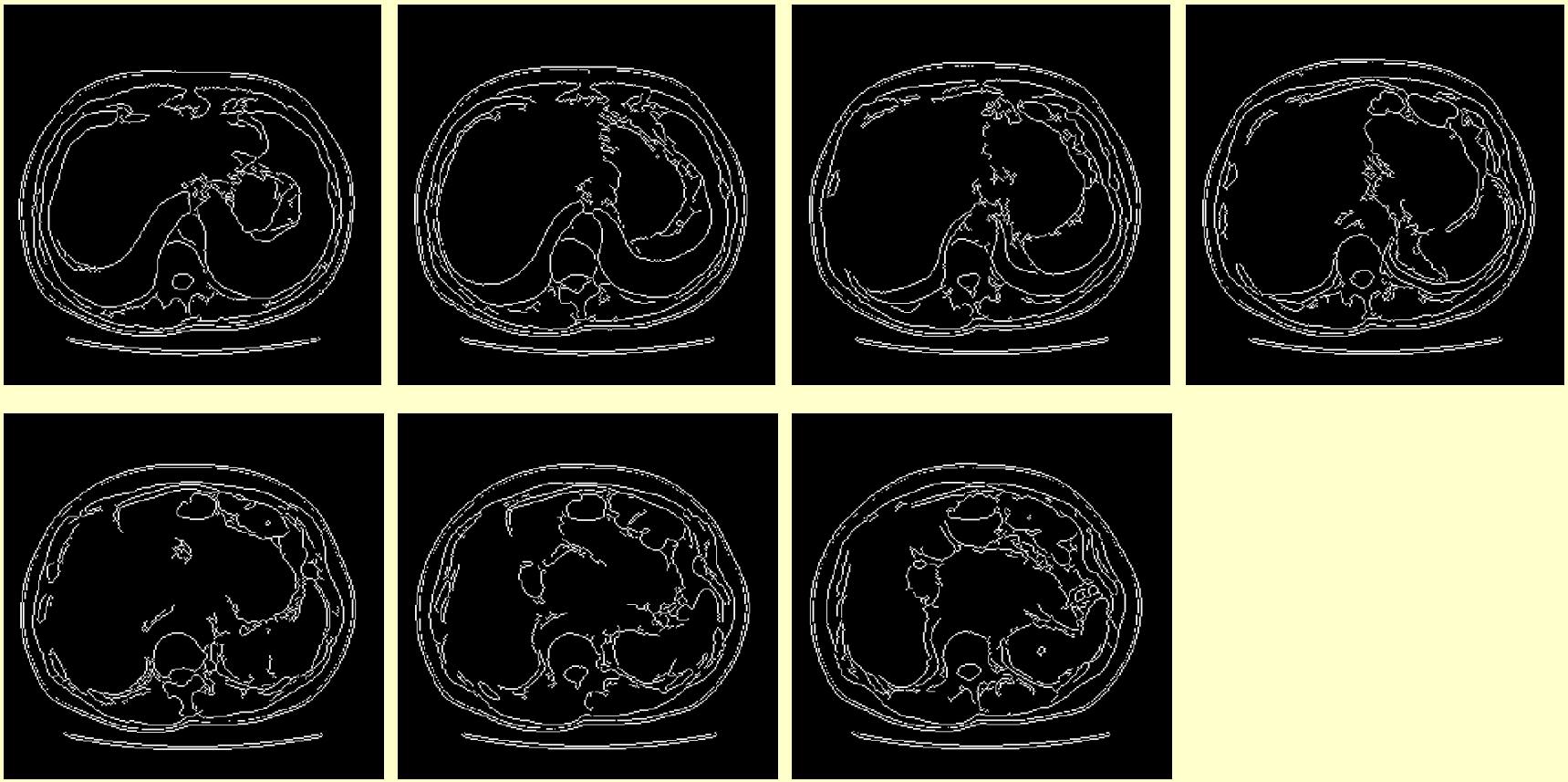

Active Contour Implementation

- Liver center estimated via ellipsoid fitting
- Local edge detection gives coarse segmentation
- 32 x 32 angular grid used for radial descriptor
- Elliptic evolving contour computed via spectral method
- Convergent to within a pixel after 5 iterations
- 3 values of α investigated:

$$\alpha = 10^{-3}, \alpha = 10^{-4}, \alpha = 10^{-6}$$

Segmentation After 5 Iterations

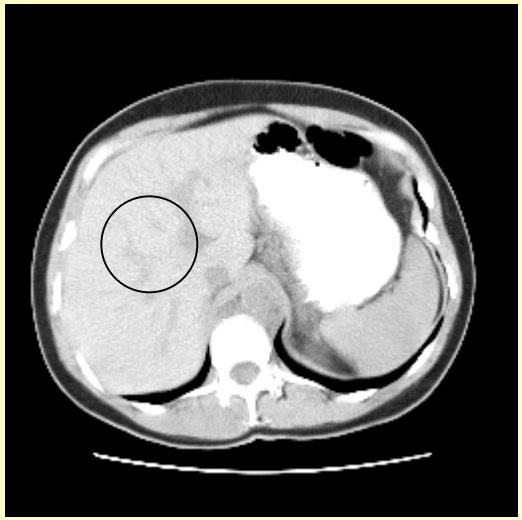

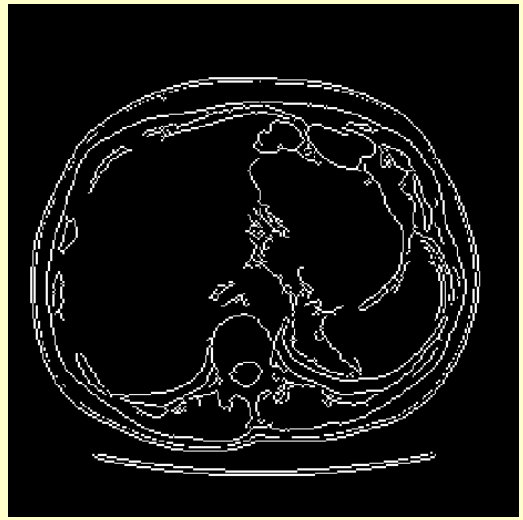

$\alpha = 10^{-3}$

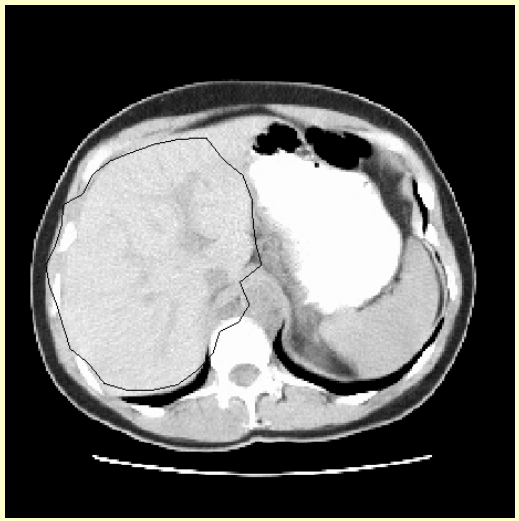

$\alpha = 10^{-4}$

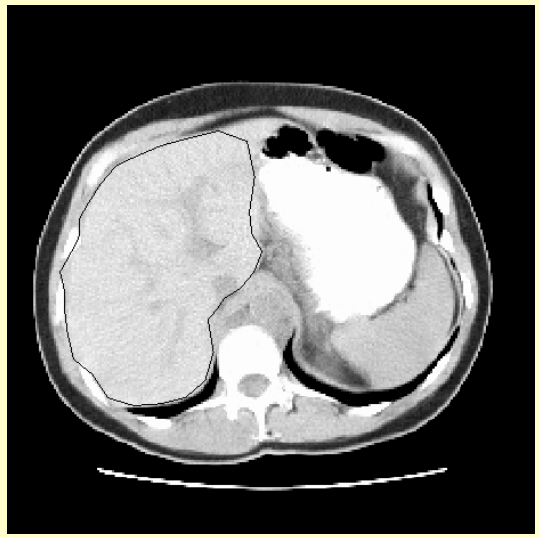

$\alpha = 10^{-6}$

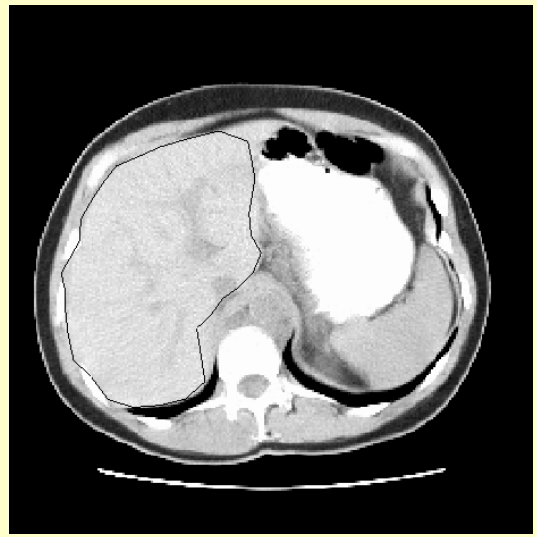

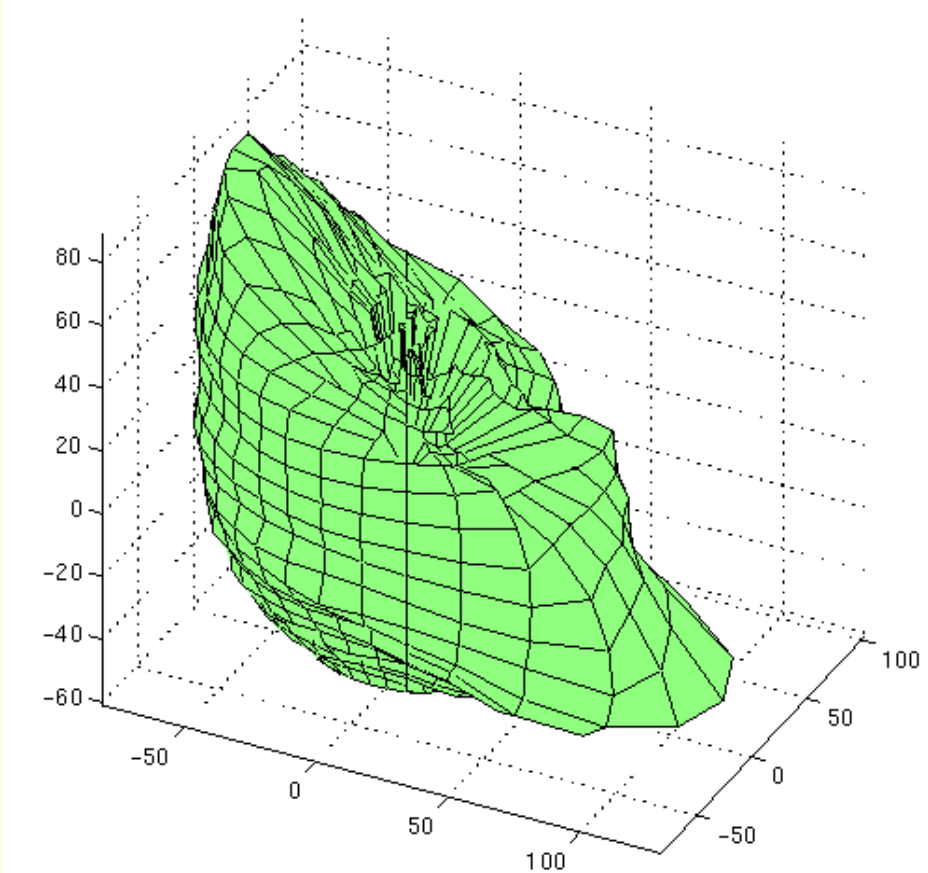

No regularization

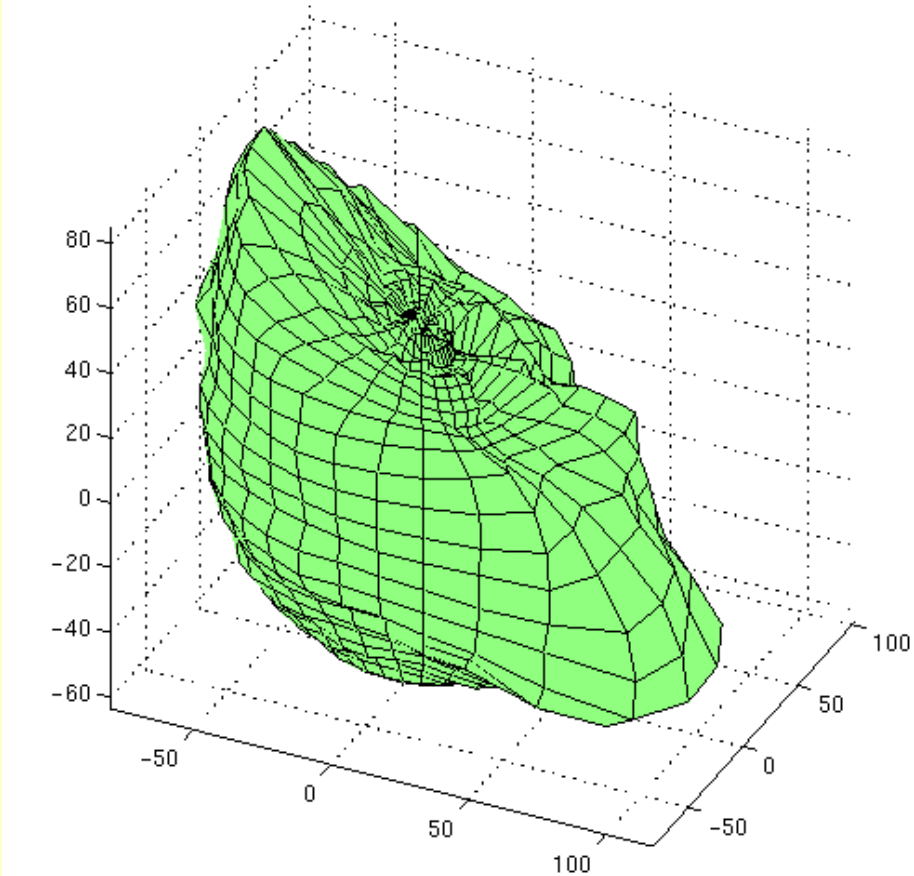

$\alpha = 10^{-4}$

Reconstruction of liver surface from 2D CT slices

Conclusions

- SH lead to optimal shape filtering and ML registration of polar 3D objects having isotropic random field models
- DFS/SH lead to spectral method for Helmholtz PDE introduced for 3D active balloons
- Application of recent advances in computational fluid dynamics to shape recovery problem
- Accelerated performance of parametric active contour on real and synthetic 3D images